AMERICAN SOCIETY FOR MICROBIOLOGY | Applied and Environmental Microbiology

Spotlight Selection | Biotechnology | Full-Length Text

Blue valorization of lignin-derived monomers via reprogramming marine bacterium *Roseovarius nubinhibens*

Ying Wei,[1] **Shu-Guang Wang,**[1,2,3] **Peng-Fei Xia**[1]

AUTHOR AFFILIATIONS See affiliation list on p. 12.

ABSTRACT Biological valorization of lignin, the second most abundant biopolymer on Earth, is an indispensable sector to build a circular economy and net-zero future. However, lignin is recalcitrant to bioupcycling, demanding innovative solutions. We report here the biological valorization of lignin-derived aromatic carbon to value-added chemicals without requesting extra organic carbon and freshwater via reprogramming the marine *Roseobacter* clade bacterium *Roseovarius nubinhibens*. We discovered the unusual advantages of this strain for the oxidation of lignin monomers and implemented a CRISPR interference (CRISPRi) system with the *lacI*-P_{trc} inducible module, nuclease-deactivated Cas9, and programmable gRNAs. This is the first CRISPR-based regulatory system in *R. nubinhibens*, enabling precise and efficient repression of genes of interest. By deploying the customized CRISPRi, we reprogrammed the carbon flux from a lignin monomer, 4-hydroxybenzoate, to achieve the maximum production of protocatechuate, a pharmaceutical compound with antibacterial, antioxidant, and anticancer properties, with minimal carbon to maintain cell growth and drive biocatalysis. As a result, we achieved a 4.89-fold increase in protocatechuate yield with a dual-targeting CRISPRi system, and the system was demonstrated with real seawater. Our work underscores the power of CRISPRi in exploiting novel microbial chassis and will accelerate the development of marine synthetic biology. Meanwhile, the introduction of a new-to-the-field lineage of marine bacteria unveils the potential of blue biotechnology leveraging resources from the ocean.

IMPORTANCE One often overlooked sector in carbon-conservative biotechnology is the water resource that sustains these enabling technologies. Similar to the "food-versus-fuel" debate, the competition of freshwater between human demands and bioproduction is another controversial issue, especially under global water scarcity. Here, we bring a new-to-the-field lineage of marine bacteria with unusual advantages to the stage of engineering biology for simultaneous carbon and water conservation. We report the valorization of lignin monomers to pharmaceutical compounds without requesting extra organic substrate (e.g., glucose) or freshwater by reprogramming the marine bacterium *Roseovarius nubinhibens* with a multiplex CRISPR interference system. Beyond the blue lignin valorization, we present a proof-of-principle of leveraging marine bacteria and engineering biology for a sustainable future.

KEYWORDS CRISPRi, marine bacteria, *Roseovarius nubinhibens*, valorization, lignin

Reverting carbon emissions back into resources for carbon-conservative bioproduction is an important route toward a net-zero future. Lignin, a prevalent aromatic polymer, represents a substantial fraction, typically ranging from 15% to 40%, of the dry mass of terrestrial plants on Earth (1–3). However, lignin is largely underutilized due to its inherent recalcitrance to biodegradation and heterogeneity in composition (4–7). Consequently, lignin-containing biomass (e.g., plant cell walls and agriculture

Editor Pablo Ivan Nikel, Danmarks Tekniske Universitet The Novo Nordisk Foundation Center for Biosustainability, Kgs. Lyngby, Denmark

Address correspondence to Peng-Fei Xia, pfxia@sdu.edu.cn.

The authors declare no conflict of interest.

See the funding table on p. 12.

Received 6 May 2024
Accepted 7 June 2024
Published 28 June 2024

wastes) often demands disposal via, for instance, incineration, causing CO_2 emission and environmental pollution. Innovations for the valorization of lignin are imperative and urgent (8). Given the revolutionary advances in engineering biology, bioconversion of lignin-derived aromatic compounds to value-added chemicals, e.g., *cis*,*cis*-muconic acids, pyridine-dicarboxylic acids, and β-ketoadipic acids, has been achieved in engineered *Pseudomonas putida* (9–11), *Corynebacterium glutamicum* (12), and *Rhodococcus jostii* (13), illustrating a promising avenue for the sustainable valorization of lignin-derived aromatics.

One often overlooked sector, however, is the source of water to sustain these enabling biotechnologies for, but not limited to, lignin valorization. A large amount of freshwater is commonly necessary to cultivate engineered microbes (14, 15), competing with human needs for freshwater. This will be a controversial issue, especially with the fact of global water scarcity (16–18). To tackle this conflict, we propose blue valorization of lignin-derived monomers, which leverages resources from the ocean including seawater and marine bacteria, to alleviate the dependence on freshwater during the biological processes (19). Marine bacteria usually survive or even thrive in environments with limited nutrients, extreme temperatures, and high salinity, which endow them with versatile metabolic capabilities and tolerances to various stressors (20–22). Besides, marine bacteria inherently grow in seawater avoiding direct competition for freshwater resources with humans. Therefore, marine bacteria can be engineered as promising microbial chassis for lignin biovalorization with seawater, resolving the challenges in carbon and water conservation simultaneously.

Roseovarius nubinhibens is a member of the marine *Roseobacter* clade with diverse metabolic capacities, including the degradation of aromatics through the β-ketoadipate pathway (23). The natural properties enable *R. nubinhibens* a potential whole-cell catalyst for the conversion of lignin-derived aromatic compounds into value-added chemicals. Though bacteria in this clade have been intensively interrogated for the ecological and evolutionary dynamics (24–26), the potential of these bacteria for biocatalysis has rarely been discovered. Notably, genetic systems are available for strain engineering, including the delivery of foreign DNAs, replicable shuttle vectors, and "knock-in" gene disruption (27–29). In a previous work, we established a CRISPR-Cas-based genome editing tool at a single-nucleotide resolution for *R. nubinhibens*, and efficient and precise gene inactivation can be realized, paving the way for the design and construction of strains capable of lignin upcycling (30).

Here, we report a customized CRISPR interference (CRISPRi) system to reprogram the marine bacterium *R. nubinhibens* for the biological valorization of lignin-derived monomers. We revealed the unusual potentials of this strain for the oxidation of the lignin-derived monomers. We modularly designed the CRISPRi system with nuclease-deactivated Cas9 (dCas9) from *Streptococcus pyogenes* and programmable gRNAs driven by an inducible system. Then, we selected 4-hydroxybenzoate (4HB) as a proof-of-principle lignin monomer and protocatechuate (PCA), a pharmaceutical compound, as the product to evaluate the bioproduction by *R. nubinhibens* with CRISPRi in both defined synthetic medium and seawater. We present here a new-to-the-field lineage of marine bacteria as whole-cell biocatalyst for lignin valorization and a paradigm of leveraging marine bacteria with cutting-edge synthetic biology tools for sustainable biorefinery. Beyond carbon, we are appealing for more attention to the water requirement of bioinnovations to ensure a sustainable future.

RESULTS

PCA accumulation during cell growth on 4-hydroxybenzoate

The protocatechuate branch of the β-ketoadipate pathway is the main pathway for the metabolism of lignin-derived aromatic molecules (31, 32). Going through this pathway, the aromatic carbon goes to the tricarboxylic acid (TCA) cycle with two key metabolites, succinyl-CoA and acetyl-CoA, as the nodes, providing carbon and energy for the anabolism and catabolism in the cell (Fig. 1A). To evaluate the potentials of

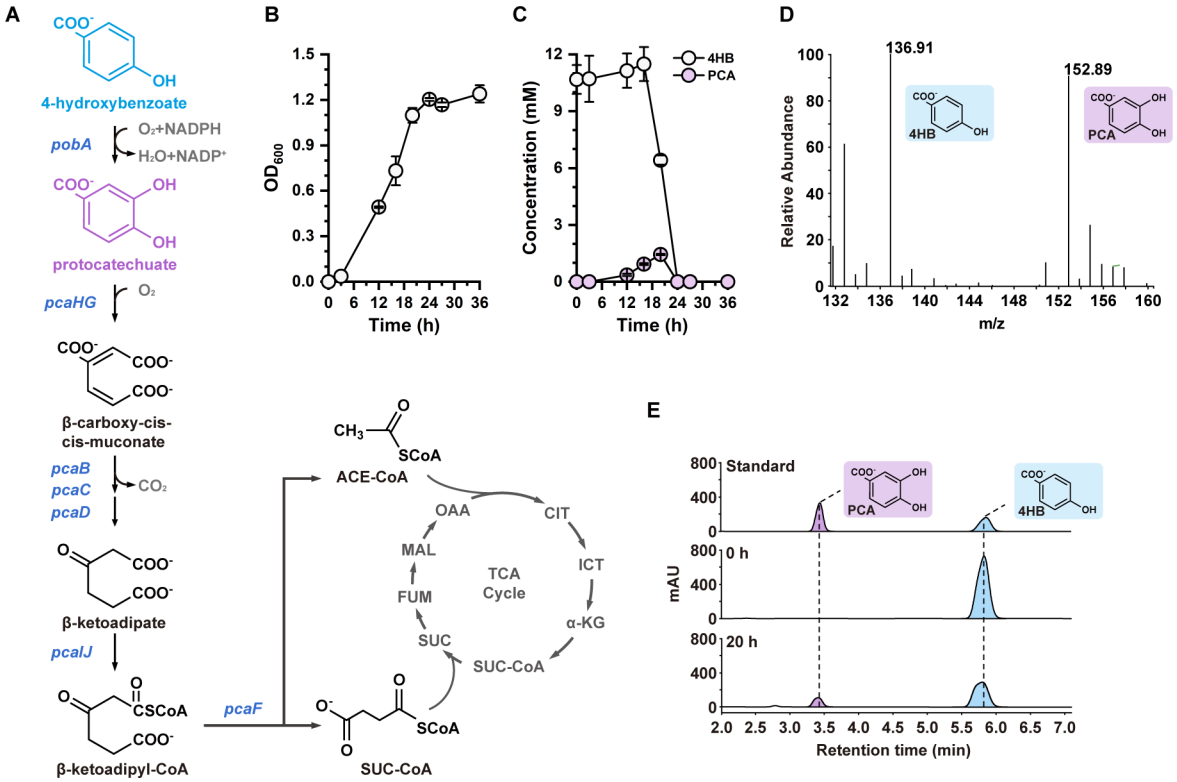

FIG 1 PCA accumulation during *R. nubinhibens* growth on 4HB. (A) The protocatechuate branch of β-ketoadipate metabolic pathway in *R. nubinhibens*. CIT, citrate; ICT, isocitrate; α-KG, alpha-ketoglutarate; SUC-CoA, succinyl-CoA; SUC, succinate; FUM, fumarate; MAL, malate; OAA, oxaloacetate; ACE-CoA, acetyl-CoA. (B) Growth profile. (C) Utilization of 4HB and accumulation of PCA in the wild-type *R. nubinhibens* with 4HB as the sole carbon source. Experiments were carried out in triplicate, and the error bars represented the standard deviations of the means of three biological replicates. (D) MS analysis of samples. (E) HPLC profile of standard and samples.

R. nubinhibens for the degradation of lignin-derived monomers, we selected 4HB, a representative and readily available lignin-derived aromatic compound monomer, as the substrate and grew the strain in a marine basal medium (MBM). Notably, *R. nubinhibens* demonstrated robust growth with 4HB as the sole carbon source without extra organic substrates, such as glucose, to power the metabolism (Fig. 1B and C). Interestingly, during the cultivation of the wild-type *R. nubinhibens* in the basal medium with 4HB, a gradual accumulation of a violet compound was observed with the growth of cells in the first 20 h (Fig. S1). Subsequent characterization via mass spectrometry (MS) and high performance liquid chromatography (HPLC) confirmed the identity of this compound as PCA (Fig. 1D and E; Fig. S2), a central metabolite in the β-ketoadipate pathway and a pharmaceutical compound with antibacterial, antioxidant, anticancer, and anti-inflammatory potentials, which has been demonstrated both *in vitro* and *in vivo* (33, 34). PCA can also be a platform compound for the production of diverse value-added compounds with significance in chemical, food, and pharmaceutical industries, such as *cis*,*cis*-muconic acid, adipic acid, and levulinic acid (35–37). However, conventional PCA production relies on extraction from plants with low yield and high cost (38). This observation implied an unusually high catalytic capability of the native 4-hydroxybenzoate 3-monooxygenase, PobA, for 4HB hydroxylation to PCA, which is usually a limiting step for aromatic utilization (39–41). Therefore, a rational allocation of carbon flux from 4HB would be possible to maximize the biosynthesis of PCA and sustain cell growth simultaneously. This can be realized using a CRISPRi system as a carbon-flux-limiting stopcock to restrain the flux toward the TCA cycle by downregulating relevant genes downstream of *pobA* (Fig. 1A).

Characterization of a *lacI*-P_{trc} inducible system in *R. nubinhibens*

One of the key advantages of CRISPRi is that the repression of target genes is tunable, which usually relies on an inducible system based on transcriptional regulators. Currently, only countable inducible systems have been reported for the *Roseobacter* clade bacteria (42), and no inducible system has been established for the marine *R. nubinhibens*. As such, we designed and constructed a *lacI*-P_{trc} inducible system consisting of the *lacI* gene coding for the repressor LacI and the corresponding promoter P_{trc} driving the expression of red fluorescent protein, mCherry, as a reporter. Without inducers, LacI would bind to the operator region of the P_{trc} promoter blocking the expression of mCherry, while, when isopropyl-β-D-thiogalactopyranoside (IPTG) is supplemented, the repressor would ligand to IPTG instead and release the promoter for the transcription of mCherry (Fig. 2A).

To assess the functionality of the *lacI*-P_{trc} inducible system, we monitored the fluorescence of *R. nubinhibens* with pmCherry (Table S1) and the control plasmid (pBBR1MCS-5; Table S1) via fluorimetry and flow cytometry. Without IPTG, both strains showed a similarly low level of background fluorescence. We tested eight different concentrations of IPTG from 0.01 to 2 mM. The strain displayed a gradually increased signal of fluorescence along with the rising concentration of IPTG from 0.01 to 0.5 mM, and the signals indicated a saturation of IPTG induction when the concentration reached 0.5 mM (Fig. 2B). The proportion of fluorescent cells reached saturation at 29.9% with 0.5 mM of IPTG (Fig. 2C and D). The partially induced cell population might result from the heterologously adapted transcriptional regulator or the distinct uptake behavior of IPTG in this marine chassis. This is the first demonstration of an inducible system in *R. nubinhibens*, making dynamic regulation of designed genetic modules possible.

Modular design of a CRISPR interference system for *R. nubinhibens*

To implement a CRISPRi system in *R. nubinhibens*, we modularly assembled the inducible module based on the *lacI*-P_{trc} system and an interference module containing *dcas9* and the gRNA cassette, carried by the pBBR1MCS-5 vector plasmid (Fig. 3A). In the design, dCas9 driven by the *lacI*-P_{trc} system reserves the ability to bind the target DNA (43–45), and navigated by a programmable gRNA, it binds to the target and sterically blocks RNA polymerase (RNAP), thereby interfering the transcription process and eventually repressing the expression of the target gene (Fig. 3B) (46–48). The gRNA cassette can be programmed for any genes of interest by substitution of the 20-nt spacer via a one-step PCR protocol (Fig. 3C).

As a proof of concept, we attempted to target two genes, *pcaC* and *pcaH,* in the genome, respectively. Both genes are involved in the β-ketoadipate pathway, which has been identified as the primary route to degrade aromatic compounds in *R. nubinhibens* (23). Specifically, the *pcaC* gene encodes the γ-carboxymuconolactone decarboxylase and *pcaH* encodes the protocatechuate 3,4-dioxygenase β-subunit catalyzing the ring cleavage together with PcaG (Fig. 1A). We constructed two working plasmids, pWYi01 (with gRNA09; Table S1) and pWYi02 (with gRNA06; Table S1) targeting *pcaC* and *pcaH*, respectively (Fig. 3D). IPTG (0.25 and 0.5 mM) were added to induce the expression of dCas9, and the expression of target genes was determined by quantitative real-time PCR (RT-qPCR). As expected, the expression of *pcaC* and *pcaH* in strains with pWYi01 or pWYi02 significantly decreased by 43.13% and 50.26%, respectively, compared to strains with the control plasmid under 0.5 mM IPTG induction (Fig. 3E and F). The repression degree with 0.5 mM IPTG was, though marginal, higher than that with 0.25 mM IPTG, implying a higher expression level of dCas9, which is in agreement with our characterization above (Fig. S3). These results demonstrated that the CRISPRi system was successfully established.

The *pcaH* and *pcaC* genes, which we targeted with CRISPRi, are located downstream of *pobA* in the *pca* gene cluster. The repression of these downstream genes is expected to promote the accumulation of upstream metabolites (Fig. 1A and 3D). So, we tested the strains with the CRISPRi system targeting *pcaH* and *pcaC*, respectively, to evaluate the

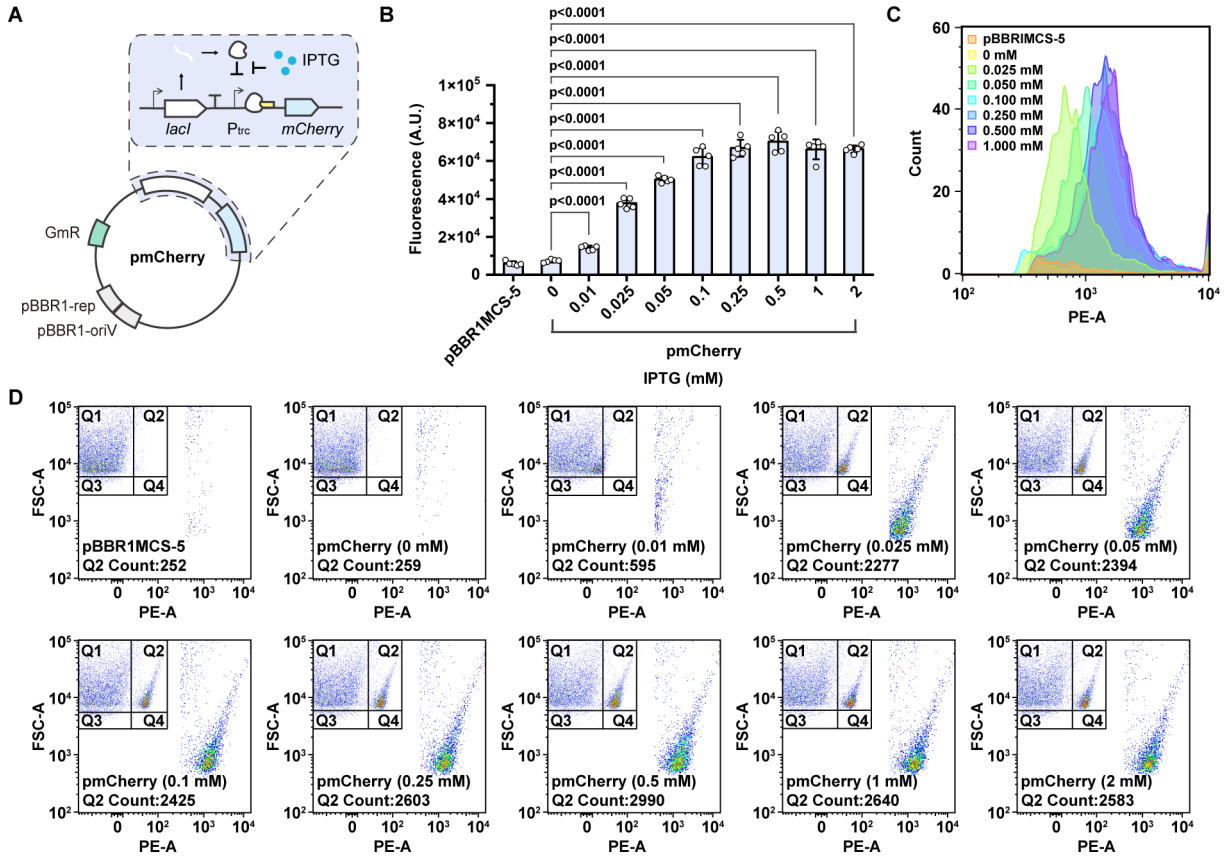

FIG 2 The *lacI*-P_{trc} inducible system for *R. nubinhibens*. (A) Schematic representation of the pmCherry. The *lacI* gene is driven by a constitutive promoter, and the mCherry fluorescence gene is driven by the P_{trc} inducible promoter. (B) Fluorescence of strains with pBBR1MCS-5, as a control, and pmCherry under different IPTG concentrations. The value of fluorescence intensity (A.U., arbitrary unit) was normalized by optical density at 600 nm with a final OD_{600} of 0.01. Experiments were carried out in quintuplicate, and the error bars represented the standard deviations of the means of five biological replicates. The differences were statistically evaluated by the *t*-test. (C) Count of mCherry fluorescent cells. (D) Distribution of mCherry fluorescent cells in the population. For each sample, 10,000 events were analyzed.

conversion of 4HB to PCA. Both strains were cultivated in shake flasks with 4HB as the sole substrate and induced with 0.5 mM IPTG. Compared with the control, both strains with CRISPRi showed slower growth rates and 4HB consumption (Fig. 3G; Fig. S4). The strain with the control plasmid pBBR1MCS-5 produced PCA at a titer of 0.46 ± 0.43 mM and a molar yield of 5.00 ± 4.69% at 36 h (Fig. 3H and I; Table S2). As expected, the strains with CRISPRi displayed higher performance with improved titer and yield of PCA. The strain expressing pWYi02 (targeting *pcaH*) exhibited a 3.85-fold increase in PCA yield, while that of the strain expressing pWYi01 (targeting *pcaC*) increased by 2.35-fold than the control strain (Fig. 3I). Specifically, the strain with CRISPRi repressing *pcaH* and *pcaC* produced 1.39 ± 0.06 and 0.97 ± 0.03 mM of PCA with a molar yield of 19.27 ± 1.93% and 11.74 ± 1.16% at 36 h, respectively (Fig. 3H and I; Table S2). Under this condition, strains with 0.25 and 0.5 mM IPTG showed similar performance in the growth rate (Fig. S5) and 4HB consumption and accumulation of PCA (Fig. S6 and S7), indicating that the difference between these two inducible strengths is marginal. These results demonstrated that the CRISPRi system efficiently allocated the carbon flux and could be modified as a powerful tool for the dynamical regulation of bioproduction in *R. nubinhibens*. However, the CRISPRi system with only one target was not sufficient, and further improvement is necessary.

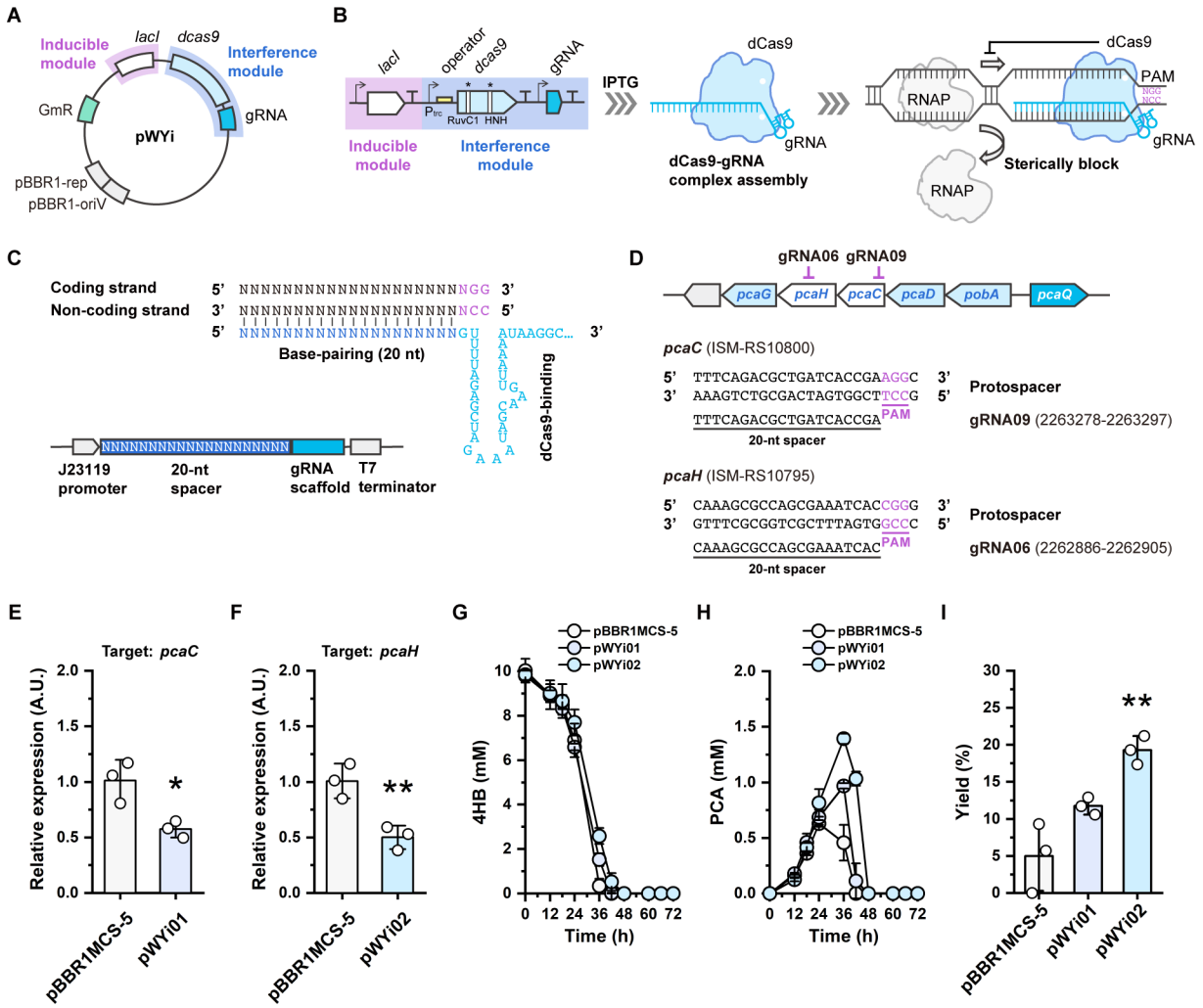

FIG 3 CRISPRi system for *R. nubinhibens*. (A) Design of the working plasmid pWYi. The pWYi plasmid was comprised of the inducible module (*lacI*-P_{trc} inducible system) and the CRISPR interference module (*dcas9* and the gRNA cassette). (B) Schematic representation of the working principle of CRISPRi. The gRNA and dCas9 (D10A and H840A) complex bind to the target DNA and sterically block the RNAP. The site of protospacer adjacent motif was highlighted in violet. (C) Structure of the gRNA cassette targeting the coding strand. The sequences of the 20-nt base-pairing region of the gRNA are identical to the coding strand. The base-pairing region was indicated in navy blue, and the dCas9 binding region was indicated in sky blue. (D) Positions of the gRNAs targeting the *pca* gene cluster. (E) Relative expression of target genes in the strain with pWYi01 and (F) pWYi02. Samples were taken at the exponential phase (OD_{600} of 0.5) with 0.5 mM IPTG, and the strain with pBBR1MCS-5 was included as the control. (G) Utilization of 4HB. (H) Titer of PCA. (I) Molar yield (%) of PCA. Experiments were carried out in triplicate, and the error bars represented the standard deviations of the means of three biological replicates. The differences were statistically evaluated by the *t*-test ($^{*}P < 0.05$; $^{**}P < 0.01$).

Multiplex CRISPRi enables enhanced biosynthesis of PCA

To further enhance the accumulation of PCA, we developed a multiplex CRISPRi system with tandem gRNA cassettes targeting different genes in the operon simultaneously. We selected *pcaG*, encoding the protocatechuate 3,4-dioxygenase α-subunit, which directly catalyzes the PCA ring-opening process together with PcaH, as another target. The tandem gRNA modules were generated by assembling two gRNA cassettes (Fig. 4A). The resulting working plasmids pWYi-M03 (with gRNA09 and gRNA06; Table S1) and pWYi-M04 (with gRNA06 and gRNA07; Table S1) target *pcaC* and *pcaH* or *pcaH* and *pcaG*, respectively (Fig. 4B). We first evaluated the expression of the target genes at the transcriptional level. As intended, all strains with CRISPRi exhibited a downregulated expression of the target genes. The expression of target genes in strains harboring the multiplex CRISPRi system was lower than that of strains with a single target (Fig. 4C and

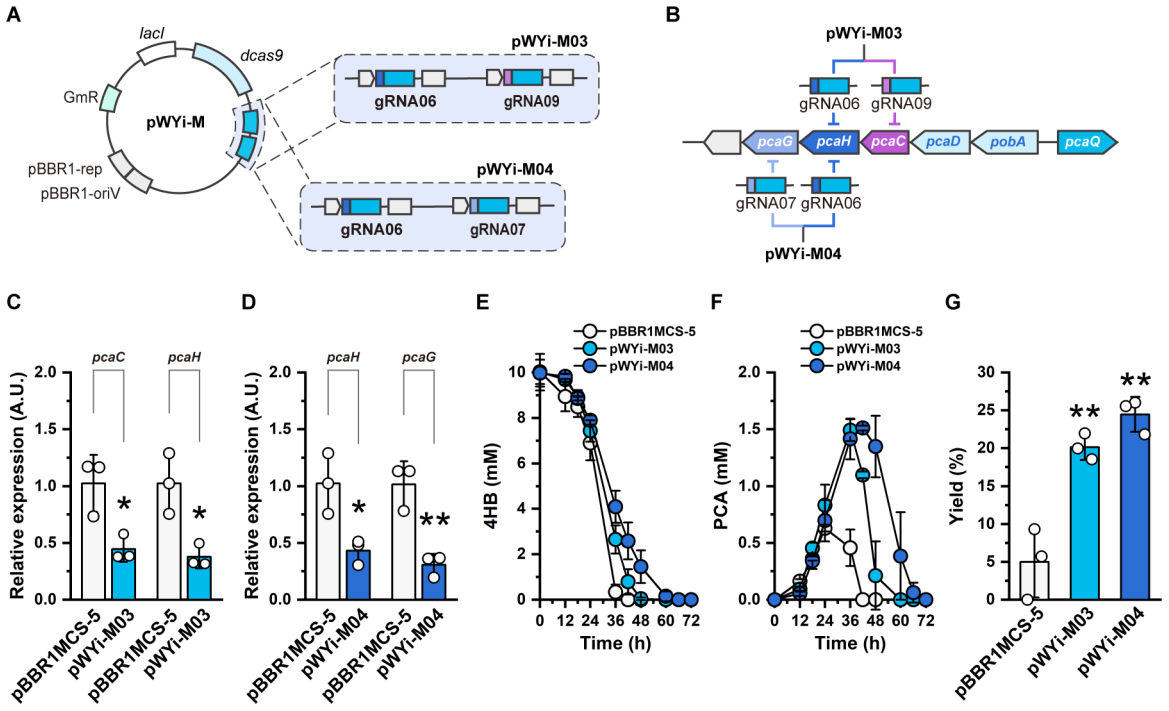

FIG 4 Multiplex CRISPRi for *R. nubinhibens*. (A) Design of pWYi-M. The multiple gRNAs module consisted of two tandem gRNA cassettes. (B) Positions of gRNAs targeting in the *pca* gene cluster. (C) Relative expression of target genes in the strain with pWYi-M03 and (D) pWYi-M04. Samples were taken at the exponential phase with 0.5 mM IPTG induction, and the strain with pBBR1MCS-5 was included as the control. (E) Utilization of 4HB. (F) Titer of PCA. (G) Molar yield (%) of PCA. Experiments were carried out in triplicate, and the error bars represented the standard deviations of the means of three biological replicates. The differences were statistically evaluated by the *t*-test ($^{*}P < 0.05$; $^{**}P < 0.01$).

D). The strain with pWYi-M03 descended the expression of *pcaC* and *pcaH* by 22.38% and 24.47%, respectively, compared to the strain with one gRNA (Fig. 4C). The multiplex CRISPRi system regulating the *pcaHG* genes displayed the strongest interference and declined the expression of *pcaH* and *pcaG* by 57.80% and 69.69% than the control, respectively (Fig. 4D). These data indicated the stronger interference of genes at the RNA level with multiple locus targeting than single sites.

With the multiplex CRISPRi system, we found that the growth of strains with all designed CRISPRi systems was repressed, while the multiplex CRISPRi targeting *pcaHG* resulted in the lowest growth rate (Fig. S8). Consistent with the growth rate, multiplex CRISPRi showed stronger interference in the utilization of 4HB than single-targeting CRISPRi (Fig. 4E; Table S3). PCA production was raised in the strain with pWYi-M03 (targeting *pcaC* and *pcaH*) at a titer of 1.49 ± 0.12 mM at 36 h, an increase of 1.54-fold and 1.07-fold over the strain with pWYi01 and pWYi02, respectively (Fig. 4F; Table S3). The maximum titer of PCA appeared in the strain harboring pWYi-M04 (targeting *pcaH* and *pcaG*) with 1.51 ± 0.03 mM at 42 h and raised 13.45-fold and 1.46-fold than the strain individually targeting *pcaC* and *pcaH*, respectively (Fig. 4F; Table S3). We calculated the molar yields of each strain at 36 h, and the strain with pWYi-M04 exhibited the highest yield at 24.47 ± 2.30%, a 2.08-fold and 1.27-fold increase over the strain with pWYi01 and pWYi02, respectively (Fig. 4G; Table S3). Yet, little improvement of the yield was observed in the strain with pWYi-M03 repressing *pcaC* and *pcaH* when compared to the strain only repressing *pcaH* alone (Tables S2 and S3). This can be explained by analyzing the β-ketoadipate pathway. PCA was catalyzed into β-carboxy-*cis*-*cis*-muconate by PcaG and PcaH. As a result, interference of these enzymes, compared to PcaC, would directly impede the aromatic ring cleavage, therefore promoting the accumulation of PCA. While the strain with the control plasmid only produced PCA with the maximum yield at 5.00 ± 4.69% at 36 h, the strain with pWYi-M04 showed an increase of 4.89-fold than the

control (Fig. 4G; Table S3). To be noticed, we also observed that all PCA produced by the control strain was consumed between 36 and 42 h. In contrast, PCA synthesized by the reprogrammed strain with pWYi-M04 was retained in the culture for 72 h. We prolonged nearly double the accumulation time of the target product compared to the control strain, providing biosynthesis with an extended time to harvest the bioproducts or terminate the process at the maximal titer of bioproducts.

Blue valorization of 4HB in real seawater

Real seawater is more complex than defined marine synthetic medium, and it is essential to evaluate our system in real seawater for blue valorization. To do so, we collected seawater in the coastal area in Qingdao city, China, and we cultivated the strain harboring pWYi-M04 with tandem gRNAs targeting *pcaH* and *pcaG* in seawater medium. Similar to the phenomenon in the defined synthetic medium, the strain with multiplex CRISPRi showed higher PCA production compared to the strain with control plasmid pBBR1MCS-5 in seawater (Fig. 5A and B; Fig. S9). As expected, the strain harboring pWYi-M04 exhibited increased PCA titer with the maximum titer at 0.92 ± 0.11 mM appearing at 60 h and raised 2.09-fold than the maximum titer of the control strain (0.44 ± 0.07 mM PCA) (Fig. 5C). In addition, our results showed that the strain with repressed *pcaH* and *pcaG* displayed higher molar yield of PCA (16.07 ± 5.29%) with a 2.10-fold increase (P = 0.09) over the control of which the yield is 7.64 ± 1.47% (Fig. 5D). Notably, the rate of 4HB consumption and PCA production in seawater medium was slower than that in marine basal medium, and we observed a slight drop of the production of PCA compared to that in the marine basal media by the same strain with pWYi-M04, which may be a result of the complexity of seawater. These results demonstrated the potential of the oceans as a water resource for bioprocesses, indicating the feasibility of blue valorization by reprogramming marine bacteria.

DISCUSSION

In this study, we report a customized CRISPRi system to reprogram the marine bacterium *R. nubinhibens* for the biological valorization of lignin-derived aromatic carbon into value-added chemicals without requesting extra organic carbon and freshwater. The strategy was demonstrated in both defined synthetic medium, such as MBM, and real seawater. Our findings highlight the unique advantages offered by *Roseobacter* clade bacteria, particularly in the context of lignin valorization. An obvious benefit is the high catalytical activity of PobA in *R. nubinhibens*, which is no longer a bottleneck but leads to the accumulation of PCA in the β-ketoadipate pathway (Fig. 1C). By using CRISPRi, we successfully targeted the key genes (*pcaC*, *pcaH,* and *pcaG*) in the β-ketoadipate pathway individually or in tandem, generating a carbon-flux-limiting stopcock for rational carbon reallocation. By doing so, we maximized the carbon accumulation before the ring-cleavage step as PCA and allowed minimal flux going to the TCA cycle to sustain cell growth and provide energy for biocatalysis. When targeting *pcaH* and *pcaG* simultaneously, the conversion of 4HB to PCA exhibited a 4.89-fold increase in molar yield (Fig. 4G), showing a great potential of the blue biovalorization of lignin monomers via the dynamic regulation of marine bacteria with multiplex CRISPRi.

This is the first report of a CRISPR-based regulatory system for the marine *Roseobacter* clade bacteria, underscoring the power of CRISPRi in exploiting novel microbial chassis (49–51). Our work also provides a paradigm of expanding cutting-edge synthetic biology tools to marine bacteria and other non-traditional microbial hosts, which are exhibiting increasingly important roles in next-generation industrial biotechnology (52–54). Nevertheless, CRISPRi cannot achieve the insertion and deletion of DNA fragments. As a result, the accumulated PCA was eventually metabolized for cell growth if it was not harvested in a certain time frame, even though our CRISPRi system expanded the operational window to around 36–48 h without sacrificing the maximum yield and titer. A combination of gene regulation and editing would be beneficial for further advances via the introduction of heterologous metabolic pathways or the termination of

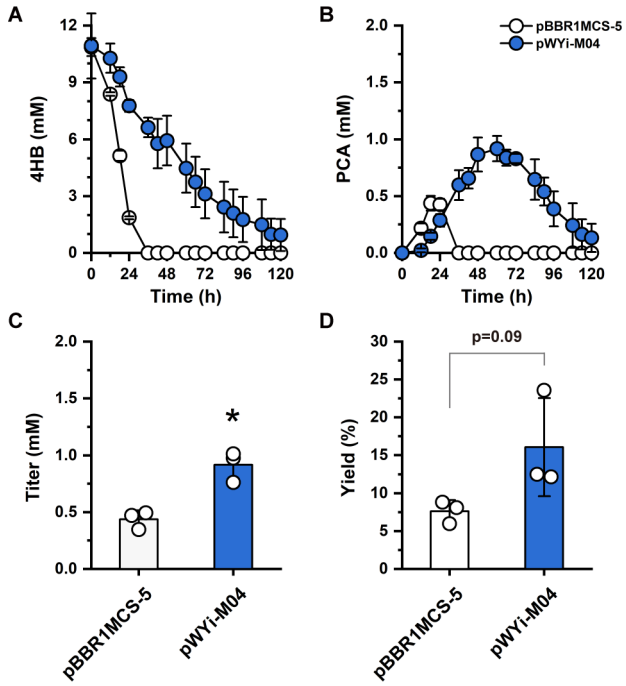

FIG 5 PCA production of the strain with pWYi-M04 in real seawater. (A) Utilization of 4HB. (B) Titer of PCA. (C) The maximum titer of PCA. (D) Molar yield (%) of PCA. Experiments were carried out in triplicate, and the error bars represented the standard deviations of the means of three biological replicates. The differences were statistically evaluated by the *t*-test ($^{*}P < 0.05$).

unwanted endogenous pathways, and *R. nubinhibens* may be further equipped with designed new features (e.g., unnatural substrates or products) for enhanced upcycling of lignin-derived monomers. Besides, we would like to acknowledge that the maximum titer of PCA of *R. nubinhibens* was lower than that of traditional microbial chassis, such as *C. glutamicum* and *P. putida*. However, members of the *Roseobacter* clade can use lignin-derived aromatic compounds as the sole carbon source without demanding any extra carbon, and most of the strains are naturally tolerant to high salinity, making it possible and preferable to use seawater for cultivation and fermentation. Finally, the development of this novel microbial chassis is only in a very early stage, and the performance would be improved significantly with the advances in synthetic biology and the understanding of its metabolisms.

Upcycling carbon lost to the environment is vital for a net-zero future. Lignin-rich biomass commonly needs conventional disposal via incineration, leading to considerable carbon loss and air pollution, for instance, the emission of greenhouse gases CO_2, NO_x, and inhalable particles (e.g., PM10 and PM2.5) (55–57). In contrast, biological valorization has been considered a carbon-efficient, economically viable, and environmentally friendly alternative to upcycle lignin to high-performance bioproducts. Two long-standing but often overlooked issues in, but not limited to, lignin biovalorization remain. One is the requirement of extra organic carbon sources, e.g., glucose, during fermentation (12, 39, 58), aggravating the "food-versus-fuel" debate. The other is the demand for water to cultivate engineered microbes, potentially rousing the competition of freshwater between humans and biosynthesis, especially under global water scarcity (59–61). Inspiringly, the development of marine microbial chassis for the valorization of lignin-derived carbon, to some extent, provides a solution to tackle these issues at once (62). We believe that blue biovalorization by engineered marine microbes will be a new wave for building a circular economy and contributing to multiple sustainable development goals (SDGs) related to the climate, carbon, and water, such as SDG6 (clean water and sanitation), SDG12 (responsible consumption and production), and SDG13

(climate action). Beyond these, blue biovalorization depending on seawater rather than the unequally distributed freshwater may also contribute to reducing inequality (SDG10) in the wave of biotechnological revolution.

MATERIALS AND METHODS

Strains and media

Escherichia coli DH5α (Takara Bio) was used for molecular cloning and cultivated in Luria–Bertani (LB) liquid media containing 10 g NaCl, 10 g tryptone, and 5 g yeast extract per liter or on LB solid agar (1.5%) plates at 37°C. When screening *E. coli* transformants and maintaining plasmids, appropriate antibiotics were added (100 µg mL^{-1} ampicillin and 20 µg mL^{-1} gentamicin). *R. nubinhibens* ISM (DSM 15170) was grown at 30°C and 180 rpm in Difco Marine Broth 2216 (MB2216) liquid media or on solid plates for general cultivation and in the MBM containing 200 mM NaCl, 50 mM $MgSO_4$, 10 mM $CaCl_2$, 10 mM KCl, 10 mM NH_4Cl, 1 mM K_2HPO_4, 0.1 mM FeEDTA, 0.05% yeast extract, and 0.1% vitamin with 10 mM 4HB as the carbon source for biosynthesis. Wolfe's Vitamin Solution (0.1%) was used in the MBM to provide vitamins for microbial growth. It contains 2.0 mg/L biotin, 2.0 mg/L folic acid, 10.0 mg/L pyridoxine hydrochloride, 5.0 mg/L thiamine·HCl, 5.0 mg/L riboflavin, 5.0 mg/L nicotinic acid, 5.0 mg/L calcium D-(+)-pantothenate, 0.1 mg/L vitamin B12, 5.0 mg/L p-aminobenzoic acid, and 5.0 mg/L thioctic acid. Seawater was collected in the coastal area at E120°69′96″ and N36°37′72″ near our campus in Qingdao city, China, and after filtration (0.22 µm), 0.05% yeast extract, 0.1% vitamin, and 10 mM 4HB were supplemented for cell growth and PCA biosynthesis. Gentamicin (20 µg mL^{-1}) was used for isolating clones of *R. nubinhibens*.

Plasmid construction and electroporation

All plasmids used in this study are summarized in Table S1, and all primers used in this study are summarized in Table S4. All the gRNA cassettes were summarized in Table S5. The synthesized sequence of mCherry is listed in Table S6. The mCherry fragment carried by pQLL plasmid with Amp^R was synthesized by Beijing Liuhe BGI and then amplified using PrimeSTAR Max DNA Polymerase (Takara Bio). The plasmid pmCherry was generated by fusing the *lacI*-P_{trc} inducible system and mCherry into the vector pBBR1MCS-5 using In-Fusion Snap Assembly Master Mix (Takara Bio). All plasmids were extracted using the QIAprep Spin Miniprep Kit (Qiagen). The gRNA09 cassette targeting *pcaC* was built via inverse PCR using back-to-back primers containing the 20 bp spacer. Based on the plasmid pWY06 (30), we constructed pWYi02 by eliminating the deaminase, and then, pWYi01 was constructed by substituting the gRNA cassette. To generate multiplex CRISPRi working plasmids, the gRNA09 and gRNA07 cassettes were assembled in the pWYi02, forming pWYi-M03 and pWYi-M03, respectively.

For the transformation of working plasmids, the electrocompetent cells were prepared by washing twice using the buffered sucrose solution and stored at −80°C before use (30). The working plasmids were added to 80 µL competent cells in a pre-cooled 0.1 cm MicroPulser Electroporation Cuvette (Bio-Rad), and the mixture was treated in MicroPulser Electroporator (Bio-Rad) at the pulse intensity of 1.8 kV and resulting pulse length of 1.3–1.5 ms. Cells after electroporation were transferred to fresh media for recovery and then plated on a solid medium supplemented with 20 µg mL^{-1} gentamicin.

Fluorimetry and flow cytometry

The strains transformed with pBBRIMCS-5 and pmCherry were cultivated overnight in MB2216 medium with 20 µg mL^{-1} gentamicin. Next, aliquots of 2 mL suspensions were induced for 4 h with IPTG at different concentrations from 0 to 2 mM. After induction, the cells were harvested and washed twice using phosphate-buffered saline. For the fluorimetry assay, the resuspended cells with an OD_{600} of 1.0 were diluted 10^2 times

to reach an OD_{600} of 0.01, and 200 µL of each bacterial suspension was transferred to 96-well microplates (Corning Costar). The OD_{600} and fluorescence intensity at an excitation wavelength of 590 nm and an emission wavelength of 645 nm were determined using Spark Multimode Microplate Reader (Tecan). The fluorescence intensity (arbitrary unit) was normalized for fair comparison. For flow cytometry, the resuspended cells were diluted by 10^3 times and then stored at 4°C until analysis. The mCherry fluorescence distribution at the population level was analyzed using BD FACS Aria Fusion (BD Biosciences) equipped with a 561 nm laser. Ten thousand single-cell events were collected for each sample. Data were processed using FlowJo (TreeStar Inc.).

Cultivation experiment

For biosynthesis, the strains from glycerol stocks were cultivated in MB2216 media overnight with appropriate antibiotics. Next, the culture was inoculated into 250 mL shake flasks containing 50 mL fresh marine basal medium with 4HB (10 mM) as the carbon source by 1:50 dilution and cultivated at 30°C and 180 rpm. Gentamicin (20 µg mL^{-1}) was added to maintain the working plasmids, and IPTG (0.25 or 0.5 mM) was supplemented for induction. Samples were taken at different intervals and stored at −20°C until analysis. OD_{600} was measured to determine the cell growth profiles of each sample. The concentration of 4HB and PCA was quantified using HPLC as described below. At least two parallel biological experiments for each strain were performed, and the mean value with standard deviation was calculated and reported.

Quantification of mRNA expression levels

After induction for 24 h, cells at the exponential phase (OD_{600} of 0.5) with the CRISPRi systems were harvested by centrifugation at 10,000 rpm and frozen with liquid nitrogen and then stored at −80°C until extraction. Total RNA was extracted using the RNAprep Pure Cell/Bacteria Kit (Tiangen) and reverse-transcribed into cDNA using the PrimeScript RT reagent Kit with gDNA Eraser (Perfect Real Time) (Takara Bio). The resulting cDNA was utilized for analysis using TB Green Premix Ex Taq II (Tli RNaseH Plus) (Takara Bio). Quantitative PCR was performed using Applied Biosystems QuantStudio 5 (Thermo Fisher Scientific). To normalize the gene expression between different samples, the gene encoding for the 16S ribosomal RNA was employed as the housekeeping gene. The primers used for RT-qPCR are listed in Table S4.

Identification and quantification of 4HB and PCA

Samples were centrifuged at 10,000 rpm for 1 min, and the supernatants were sterilely filtered by 0.22 µm filter and diluted 10 times. For the identification of products, samples were demineralized by solid phase extraction using HyperSep C18 (Thermo Scientific) and analyzed using HPLC-MS (LCQ Fleet, Thermo Fisher Scientific). For quantification of 4HB and PCA, samples were detected by Agilent 1260 HPLC equipped with a UV detector (Agilent Technologies) at a wavelength of 210 nm with an injection volume of 10 µL. Chromatographic separation was realized by an EC-C18 column 4 µm, 4.6 × 100 µm (Agilent Technologies) at 25°C with the mobile phase comprised of 90% formic acid (0.1%) and 10% acetonitrile at a constant flow rate of 0.8 mL per min. The molar yield (%) of PCA was calculated by dividing the titers of PCA by 4HB.

ACKNOWLEDGMENTS

The authors thank Dr. Haiyan Yu for the assistance with flow cytometry analysis and Dr. Fanping Zhu for the help with HPLC-MS analysis. This work was supported by the National Natural Science Foundation of China (22278246, U20A20146, and 22378233), the Department of Science and Technology of Shandong Province (2022HWYQ-017), the Natural Science Foundation of Shandong Province (ZR2021ME066), the Qilu Young Scholar Program of Shandong University (to P.-F.X.), and the Taishan Scholars Project of Shandong Province (No. tstp20230604).

AUTHOR AFFILIATIONS

[1]School of Environmental Science and Engineering, Shandong University, Qingdao, China
[2]Sino-French Research Institute for Ecology and Environment, Shandong University, Qingdao, China
[3]Weihai Research Institute of Industrial Technology, Shandong University, Weihai, China

AUTHOR ORCIDs

Peng-Fei Xia http://orcid.org/0000-0001-5881-9834

FUNDING

Funder	Grant(s)	Author(s)
MOST | National Natural Science Foundation of China (NSFC)	22278246	Peng-Fei Xia
MOST | National Natural Science Foundation of China (NSFC)	U20A20146, 22378233	Shu-Guang Wang
Department of Science and Technology of Shandong Province	2022HWYQ-017	Peng-Fei Xia
National Science Foundation of Shandong Province	ZR2021ME066	Peng-Fei Xia
Shandong University (SDU)	Qilu Young Scholar Program	Peng-Fei Xia
Taishan Scholars Project of Shandong Province	tstp20230604	Shu-Guang Wang

ADDITIONAL FILES

The following material is available online.

Supplemental Material

Supplemental material (AEM00890-24-S0001.pdf). Tables S1 to S6; Figures S1 to S9.

REFERENCES

1. Bugg TDH, Ahmad M, Hardiman EM, Rahmanpour R. 2011. Pathways for degradation of lignin in bacteria and fungi. Nat Prod Rep 28:1883–1896. https://doi.org/10.1039/c1np00042j
2. Dong L, Wang Y, Dong Y, Zhang Y, Pan M, Liu X, Gu X, Antonietti M, Chen Z. 2023. Sustainable production of dopamine hydrochloride from softwood lignin. Nat Commun 14:4996. https://doi.org/10.1038/s41467-023-40702-2
3. Lan HN, Liu RY, Liu ZH, Li X, Li BZ, Yuan YJ. 2023. Biological valorization of lignin to flavonoids. Biotechnol Adv 64:108107. https://doi.org/10.1016/j.biotechadv.2023.108107
4. Beckham GT, Johnson CW, Karp EM, Salvachúa D, Vardon DR. 2016. Opportunities and challenges in biological lignin valorization. Curr Opin Biotechnol 42:40–53. https://doi.org/10.1016/j.copbio.2016.02.030
5. De Wild PJ, Huijgen WJJ, Gosselink RJA. 2014. Lignin pyrolysis for profitable lignocellulosic biorefineries. Biofuels Bioprod Bioref 8:645–657. https://doi.org/10.1002/bbb.1474
6. Wu X, Fan X, Xie S, Lin J, Cheng J, Zhang Q, Chen L, Wang Y. 2018. Solar energy-driven lignin-first approach to full utilization of lignocellulosic biomass under mild conditions. Nat Catal 1:772–780. https://doi.org/10.1038/s41929-018-0148-8
7. Liu ZH, Hao N, Wang YY, Dou C, Lin F, Shen R, Bura R, Hodge DB, Dale BE, Ragauskas AJ, Yang B, Yuan JS. 2021. Transforming biorefinery designs with 'plug-in processes of lignin' to enable economic waste valorization. Nat Commun 12:3912. https://doi.org/10.1038/s41467-021-23920-4
8. Liu ZH, Li BZ, Yuan JS, Yuan YJ. 2022. Creative biological Lignin conversion routes toward lignin valorization. Trends Biotechnol 40:1550–1566. https://doi.org/10.1016/j.tibtech.2022.09.014
9. Johnson CW, Salvachúa D, Rorrer NA, Black BA, Vardon DR, St. John PC, Cleveland NS, Dominick G, Elmore JR, Grundl N, Khanna P, Martinez CR, Michener WE, Peterson DJ, Ramirez KJ, Singh P, VanderWall TA, Wilson AN, Yi X, Biddy MJ, Bomble YJ, Guss AM, Beckham GT. 2019. Innovative chemicals and materials from bacterial aromatic catabolic pathways. Joule 3:1523–1537. https://doi.org/10.1016/j.joule.2019.05.011
10. Ling C, Peabody GL, Salvachúa D, Kim Y-M, Kneucker CM, Calvey CH, Monninger MA, Munoz NM, Poirier BC, Ramirez KJ, St John PC, Woodworth SP, Magnuson JK, Burnum-Johnson KE, Guss AM, Johnson CW, Beckham GT. 2022. Muconic acid production from glucose and xylose in *Pseudomonas putida* via evolution and metabolic engineering. Nat Commun 13:4925. https://doi.org/10.1038/s41467-022-32296-y
11. Werner AZ, Cordell WT, Lahive CW, Klein BC, Singer CA, Tan ECD, Ingraham MA, Ramirez KJ, Kim DH, Pedersen JN, Johnson CW, Pfleger BF, Beckham GT, Salvachúa D. 2023. Lignin conversion to β-Ketoadipic acid by *Pseudomonas putida* via metabolic engineering and bioprocess development. Sci Adv 9:eadj0053. https://doi.org/10.1126/sciadv.adj0053
12. Weiland F, Barton N, Kohlstedt M, Becker J, Wittmann C. 2023. Systems metabolic engineering upgrades *Corynebacterium glutamicum* to high-efficiency *cis,cis*-muconic acid production from lignin-based aromatics. Metab Eng 75:153–169. https://doi.org/10.1016/j.ymben.2022.12.005

13. Spence EM, Calvo-Bado L, Mines P, Bugg TDH. 2021. Metabolic engineering of *Rhodococcus jostii* RHA1 for production of pyridine-dicarboxylic acids from lignin. Microb Cell Fact 20:15. https://doi.org/10.1186/s12934-020-01504-z
14. Ye JW, Lin YN, Yi XQ, Yu ZX, Liu X, Chen GQ. 2023. Synthetic biology of extremophiles: a new wave of biomanufacturing. Trends Biotechnol 41:342–357. https://doi.org/10.1016/j.tibtech.2022.11.010
15. Chen GQ, Jiang XR. 2018. Next generation industrial biotechnology based on extremophilic bacteria. Curr Opin Biotechnol 50:94–100. https://doi.org/10.1016/j.copbio.2017.11.016
16. Scanlon BR, Fakhreddine S, Rateb A, de Graaf I, Famiglietti J, Gleeson T, Grafton RQ, Jobbagy E, Kebede S, Kolusu SR, Konikow LF, Long D, Mekonnen M, Schmied HM, Mukherjee A, MacDonald A, Reedy RC, Shamsudduha M, Simmons CT, Sun A, Taylor RG, Villholth KG, Vörösmarty CJ, Zheng C. 2023. Global water resources and the role of groundwater in a resilient water future. Nat Rev Earth Environ 4:87–101. https://doi.org/10.1038/s43017-022-00378-6
17. Schyns JF, Hoekstra AY, Booij MJ, Hogeboom RJ, Mekonnen MM. 2019. Limits to the world's green water resources for food, feed, fiber, timber, and bioenergy. Proc Natl Acad Sci U S A 116:4893–4898. https://doi.org/10.1073/pnas.1817380116
18. Liu J, Yang H, Gosling SN, Kummu M, Flörke M, Pfister S, Hanasaki N, Wada Y, Zhang X, Zheng C, Alcamo J, Oki T. 2017. Water scarcity assessments in the past, present and future. Earths Future 5:545–559. https://doi.org/10.1002/2016EF000518
19. Paoli L, Ruscheweyh H-J, Forneris CC, Hubrich F, Kautsar S, Bhushan A, Lotti A, Clayssen Q, Salazar G, Milanese A, et al. 2022. Biosynthetic potential of the global ocean microbiome. Nature 607:111–118. https://doi.org/10.1038/s41586-022-04862-3
20. Zhou Q, Hotta K, Deng Y, Yuan R, Quan S, Chen X. 2021. Advances in biosynthesis of natural products from marine microorganisms. Microorganisms 9:2551. https://doi.org/10.3390/microorganisms9122551
21. Lyu C, Chen T, Qiang B, Liu N, Wang H, Zhang L, Liu Z. 2021. CMNPD: a comprehensive marine natural products database towards facilitating drug discovery from the ocean. Nucleic Acids Res 49:D509–D515. https://doi.org/10.1093/nar/gkaa763
22. Imhoff JF, Labes A, Wiese J. 2011. Bio-mining the microbial treasures of the ocean: new natural products. Biotechnol Adv 29:468–482. https://doi.org/10.1016/j.biotechadv.2011.03.001
23. Buchan A, Neidle EL, Moran MA. 2004. Diverse organization of genes of the β-ketoadipate pathway in members of the marine *Roseobacter* lineage. Appl Environ Microbiol 70:1658–1668. https://doi.org/10.1128/AEM.70.3.1658-1668.2004
24. Moran MA, Belas R, Schell MA, González JM, Sun F, Sun S, Binder BJ, Edmonds J, Ye W, Orcutt B, Howard EC, Meile C, Palefsky W, Goesmann A, Ren Q, Paulsen I, Ulrich LE, Thompson LS, Saunders E, Buchan A. 2007. Ecological genomics of marine *Roseobacters*. Appl Environ Microbiol 73:4559–4569. https://doi.org/10.1128/AEM.02580-06
25. Luo H, Moran MA. 2014. Evolutionary ecology of the marine *Roseobacter* clade. Microbiol Mol Biol Rev 78:573–587. https://doi.org/10.1128/MMBR.00020-14
26. Chu X, Li S, Wang S, Luo D, Luo H. 2021. Gene loss through pseudogenization contributes to the ecological diversification of a generalist *Roseobacter* lineage. ISME J 15:489–502. https://doi.org/10.1038/s41396-020-00790-0
27. Piekarski T, Buchholz I, Drepper T, Schobert M, Wagner-Doebler I, Tielen P, Jahn D. 2009. Genetic tools for the investigation of *Roseobacter* clade bacteria. BMC Microbiol 9:265. https://doi.org/10.1186/1471-2180-9-265
28. Smith AF, Rihtman B, Stirrup R, Silvano E, Mausz MA, Scanlan DJ, Chen Y. 2019. Elucidation of glutamine lipid biosynthesis in marine bacteria reveals its importance under phosphorus deplete growth in *Rhodobacteraceae*. ISME J 13:39–49. https://doi.org/10.1038/s41396-018-0249-z
29. Li C-Y, Mausz MA, Murphy A, Zhang N, Chen X-L, Wang S-Y, Gao C, Aguilo-Ferretjans MM, Silvano E, Lidbury IDEA, Fu H-H, Todd JD, Chen Y, Zhang Y-Z. 2023. Ubiquitous occurrence of a dimethylsulfoniopropionate ABC transporter in abundant marine bacteria. ISME J 17:579–587. https://doi.org/10.1038/s41396-023-01375-3
30. Wei Y, Feng LJ, Yuan XZ, Wang SG, Xia PF. 2023. Developing a base editing system for marine *Roseobacter* clade bacteria. ACS Synth Biol 12:2178–2186. https://doi.org/10.1021/acssynbio.3c00259
31. Alejandro-Marín CM, Bosch R, Nogales B. 2014. Comparative genomics of the protocatechuate branch of the β-ketoadipate pathway in the *Roseobacter* lineage. Mar Genomics 17:25–33. https://doi.org/10.1016/j.margen.2014.05.008
32. Yamanashi T, Kim SY, Hara H, Funa N. 2015. In vitro reconstitution of the catabolic reactions catalyzed by PcaHG, PcaB, and PcaL: the protocatechuate branch of the β-ketoadipate pathway in *Rhodococcus jostii* RHA1. Biosci Biotechnol Biochem 79:830–835. https://doi.org/10.1080/09168451.2014.993915
33. Krzysztoforska K, Mirowska-Guzel D, Widy-Tyszkiewicz E. 2019. Pharmacological effects of protocatechuic acid and its therapeutic potential in neurodegenerative diseases: review on the basis of *in vitro* and *in vivo* studies in rodents and humans. Nutr Neurosci 22:72–82. https://doi.org/10.1080/1028415X.2017.1354543
34. Song J, He Y, Luo C, Feng B, Ran F, Xu H, Ci Z, Xu R, Han L, Zhang D. 2020. New progress in the pharmacology of protocatechuic acid: a compound ingested in daily foods and herbs frequently and heavily. Pharmacol Res 161:105109. https://doi.org/10.1016/j.phrs.2020.105109
35. Shanks BH, Keeling PL. 2017. Bioprivileged molecules: creating value from biomass. Green Chem 19:3177–3185. https://doi.org/10.1039/C7GC00296C
36. Lo TM, Hwang IY, Cho HS, Fedora RE, Chng SH, Choi WJ, Chang MW. 2021. Biosynthesis of commodity chemicals from oil palm empty fruit bunch lignin. Front Microbiol 12:663642. https://doi.org/10.3389/fmicb.2021.663642
37. Kohlstedt M, Starck S, Barton N, Stolzenberger J, Selzer M, Mehlmann K, Schneider R, Pleissner D, Rinkel J, Dickschat JS, Venus J, B J H van Duuren J, Wittmann C. 2018. From lignin to nylon: cascaded chemical and biochemical conversion using metabolically engineered *Pseudomonas putida*. Metab Eng 47:279–293. https://doi.org/10.1016/j.ymben.2018.03.003
38. Kogure T, Suda M, Hiraga K, Inui M. 2021. Protocatechuate overproduction by *Corynebacterium glutamicum* via simultaneous engineering of native and heterologous biosynthetic pathways. Metab Eng 65:232–242. https://doi.org/10.1016/j.ymben.2020.11.007
39. Kuatsjah E, Johnson CW, Salvachúa D, Werner AZ, Zahn M, Szostkiewicz CJ, Singer CA, Dominick G, Okekeogbu I, Haugen SJ, Woodworth SP, Ramirez KJ, Giannone RJ, Hettich RL, McGeehan JE, Beckham GT. 2022. Debottlenecking 4-hydroxybenzoate hydroxylation in *Pseudomonas putida* KT2440 improves muconate productivity from p-coumarate. Metab Eng 70:31–42. https://doi.org/10.1016/j.ymben.2021.12.010
40. Salvachúa D, Johnson CW, Singer CA, Rohrer H, Peterson DJ, Black BA, Knapp A, Beckham GT. 2018. Bioprocess development for muconic acid production from aromatic compounds and lignin. Green Chem 20:5007–5019. https://doi.org/10.1039/C8GC02519C
41. Sonoki T, Morooka M, Sakamoto K, Otsuka Y, Nakamura M, Jellison J, Goodell B. 2014. Enhancement of protocatechuate decarboxylase activity for the effective production of muconate from lignin-related aromatic compounds. J Biotechnol 192:71–77. https://doi.org/10.1016/j.jbiotec.2014.10.027
42. Schuster LA, Reisch CR. 2021. A plasmid toolbox for controlled gene expression across the proteobacteria. Nucleic Acids Res 49:7189–7202. https://doi.org/10.1093/nar/gkab496
43. Larson MH, Gilbert LA, Wang X, Lim WA, Weissman JS, Qi LS. 2013. CRISPR interference (CRISPRi) for sequence-specific control of gene expression. Nat Protoc 8:2180–2196. https://doi.org/10.1038/nprot.2013.132
44. Wu J, Cheng ZH, Min D, Cheng L, He RL, Liu DF, Li WW. 2020. CRISPRi system as an efficient, simple platform for rapid identification of genes involved in pollutant transformation by *Aeromonas hydrophila*. Environ Sci Technol 54:3306–3315. https://doi.org/10.1021/acs.est.9b07191
45. Huang H-H, Bellato M, Qian Y, Cárdenas P, Pasotti L, Magni P, Del Vecchio D. 2021. dCas9 regulator to neutralize competition in CRISPRi circuits. Nat Commun 12:1692. https://doi.org/10.1038/s41467-021-21772-6
46. Todor H, Silvis MR, Osadnik H, Gross CA. 2021. Bacterial CRISPR screens for gene function. Curr Opin Microbiol 59:102–109. https://doi.org/10.1016/j.mib.2020.11.005
47. Peters JM, Koo BM, Patino R, Heussler GE, Hearne CC, Qu J, Inclan YF, Hawkins JS, Lu CHS, Silvis MR, Harden MM, Osadnik H, Peters JE, Engel JN, Dutton RJ, Grossman AD, Gross CA, Rosenberg OS. 2019. Enabling

genetic analysis of diverse bacteria with mobile-CRISPRi. Nat Microbiol 4:244–250. https://doi.org/10.1038/s41564-018-0327-z
48. Liu Y, Pinto F, Wan X, Yang Z, Peng S, Li M, Cooper JM, Xie Z, French CE, Wang B. 2022. Reprogrammed tracrRNAs enable repurposing of RNAs as crRNAs and sequence-specific RNA biosensors. Nat Commun 13:1937. https://doi.org/10.1038/s41467-022-29604-x
49. Kozaeva E, Nielsen ZS, Nieto-Domínguez M, Nikel PI. 2024. The pAblo.pCasso self-curing vector toolset for unconstrained cytidine and adenine base-editing in Gram-negative bacteria. Nucleic Acids Res 52:e19. https://doi.org/10.1093/nar/gkad1236
50. Martínez-García E, Fraile S, Algar E, Aparicio T, Velázquez E, Calles B, Tas H, Blázquez B, Martín B, Prieto C, Sánchez-Sampedro L, Nørholm MHH, Volke DC, Wirth NT, Dvořák P, Alejaldre L, Grozinger L, Crowther M, Goñi-Moreno A, Nikel PI, Nogales J, deLorenzo V. 2023. SEVA 4.0: an update of the standard European vector architecture database for advanced analysis and programming of bacterial phenotypes. Nucleic Acids Research 51:D1558–D1567. https://doi.org/10.1093/nar/gkac1059
51. Volke DC, Orsi E, Nikel PI. 2023. Emergent CRISPR-Cas-based technologies for engineering non-model bacteria. Curr Opin Microbiol 75:102353. https://doi.org/10.1016/j.mib.2023.102353
52. Chen Y, Chen XY, Du HT, Zhang X, Ma YM, Chen JC, Ye JW, Jiang XR, Chen GQ. 2019. Chromosome engineering of the TCA cycle in *Halomonas bluephagenesis* for production of copolymers of 3-hydroxybutyrate and 3-hydroxyvalerate (PHBV). Metab Eng 54:69–82. https://doi.org/10.1016/j.ymben.2019.03.006
53. Jiang XR, Yan X, Yu LP, Liu XY, Chen GQ. 2021. Hyperproduction of 3-hydroxypropionate by *Halomonas bluephagenesis*. Nat Commun 12:1513. https://doi.org/10.1038/s41467-021-21632-3
54. Wang Z, Qin Q, Zheng Y, Li F, Zhao Y, Chen GQ. 2021. Engineering the permeability of *Halomonas bluephagenesis* enhanced its chassis properties. Metab Eng 67:53–66. https://doi.org/10.1016/j.ymben.2021.05.010
55. Ragauskas AJ, Beckham GT, Biddy MJ, Chandra R, Chen F, Davis MF, Davison BH, Dixon RA, Gilna P, Keller M, Langan P, Naskar AK, Saddler JN, Tschaplinski TJ, Tuskan GA, Wyman CE. 2014. Lignin valorization: improving lignin processing in the biorefinery. Science 344:1246843. https://doi.org/10.1126/science.1246843
56. Liu Q, Kawai T, Inukai Y, Aoki D, Feng Z, Xiao Y, Fukushima K, Lin X, Shi W, Busch W, Matsushita Y, Li B. 2023. A lignin-derived material improves plant nutrient bioavailability and growth through its metal chelating capacity. Nat Commun 14:4866. https://doi.org/10.1038/s41467-023-40497-2
57. Choi SY, Lee Y, Yu HE, Cho IJ, Kang M, Lee SY. 2023. Sustainable production and degradation of plastics using microbes. Nat Microbiol 8:2253–2276. https://doi.org/10.1038/s41564-023-01529-1
58. Johnson CW, Salvachúa D, Khanna P, Smith H, Peterson DJ, Beckham GT. 2016. Enhancing muconic acid production from glucose and lignin-derived aromatic compounds via increased protocatechuate decarboxylase activity. Metab Eng Commun 3:111–119. https://doi.org/10.1016/j.meteno.2016.04.002
59. Greve P, Kahil T, Mochizuki J, Schinko T, Satoh Y, Burek P, Fischer G, Tramberend S, Burtscher R, Langan S, Wada Y. 2018. Global assessment of water challenges under uncertainty in water scarcity projections. Nat Sustain 1:486–494. https://doi.org/10.1038/s41893-018-0134-9
60. He C, Liu Z, Wu J, Pan X, Fang Z, Li J, Bryan BA. 2021. Future global urban water scarcity and potential solutions. Nat Commun 12:4667. https://doi.org/10.1038/s41467-021-25026-3
61. Yoon J, Klassert C, Selby P, Lachaut T, Knox S, Avisse N, Harou J, Tilmant A, Klauer B, Mustafa D, Sigel K, Talozi S, Gawel E, Medellín-Azuara J, Bataineh B, Zhang H, Gorelick SM. 2021. A coupled human-natural system analysis of freshwater security under climate and population change. Proc Natl Acad Sci U S A 118:e2020431118. https://doi.org/10.1073/pnas.2020431118
62. Schada von Borzyskowski L. 2023. Taking synthetic biology to the seas: from blue chassis organisms to marine aquaforming. ChemBioChem 24:e202200786. https://doi.org/10.1002/cbic.202200786